minerals

MDPI

Article

Age and Depositional Temperature of Quaternary Travertine Spring Mounds from Slovakia

Daniella S. C. Vieira [1,2], Daniel Pivko [3], László Rinyu [4], László Palcsu [4], Gabriella I. Kiss [4], Hsun-Ming Hu [5,6,7], Chuan-Chou Shen [6,7] and Sándor Kele [2,8,*]

1 Institute of Geography and Earth Sciences, Faculty of Science, Eötvös Loránd University, 1117 Budapest, Hungary; daniellacvieirah@gmail.com
2 Research Centre for Astronomy and Earth Sciences, Institute for Geological and Geochemical Research, Eötvös Loránd Research Network, Budaörsi út 45, 1112 Budapest, Hungary
3 Department of Geology and Paleontology, Faculty of Natural Sciences, Comenius University, Ilkovičova 6, 842 15 Bratislava, Slovakia; daniel.pivko@uniba.sk
4 Isotope Climatology and Environmental Research Centre (ICER), Institute for Nuclear Research, Eötvös Loránd Research Network, Bem tér 18/c, 4026 Debrecen, Hungary; rinyu.laszlo@atomki.hu (L.R.); palcsu.laszlo@atomki.hu (L.P.); kiss.gabriella@atomki.hu (G.I.K.)
5 Radiogenic Isotope Facility, School of Earth and Environmental Sciences, The University of Queensland, Brisbane, QLD 4072, Australia; hsunming.hu@gmail.com
6 High-Precision Mass Spectrometry and Environment Change Laboratory (HISPEC), Department of Geosciences, National Taiwan University, Taipei 10617, Taiwan; river@ntu.edu.tw
7 Research Center for Future Earth, National Taiwan University, Taipei 10617, Taiwan
8 CSFK, MTA Centre of Excellence, Konkoly Thege Miklós út 15-17, 1121 Budapest, Hungary
* Correspondence: kele.sandor@csfk.org

Abstract: Travertine spring mounds are common in Slovakia; however, their age and depositional temperature are still poorly known. Our study is the first multimethodological investigation involving stable carbon, oxygen, and clumped isotope (Δ_{47}) analyses and U-Th age determination of travertine mounds from different locations in Slovakia (Santovka, Dudince, Čerin, Bešeňová, Liptovský Ján, Liptovské Sliače, Vyšné Ružbachy, Gánovce, and Sivá Brada) to provide information about their age, origin, precipitation conditions, and temperature. The positive $\delta^{13}C$ values imply that the parent water was charged with heavy CO_2 of deep origin. The $\delta^{18}O$ values of spring waters range between −11.4‰ and −8.9‰, whereas the $\delta^{2}H$ values vary from −80.5‰ to −58.3, indicating a meteoric origin for spring waters. Clumped isotope compositions (Δ_{47}) correspond to a deposition temperature between 4 °C and 32 °C. The U-Th age data of the studied travertines vary from 1.2 (Liptovské Sliače) to 301 ka (Dudince). Our results can serve as a basis for further detailed geochronological and geochemical studies to reconstruct the paleoclimate and paleoenvironment during travertine deposition periods in Slovakia since the mid-Pleistocene transition.

Keywords: travertine spring mounds; Slovakia; stable and clumped isotopes; U-Th dating

Citation: Vieira, D.S.C.; Pivko, D.; Rinyu, L.; Palcsu, L.; Kiss, G.I.; Hu, H.-M.; Shen, C.-C.; Kele, S. Age and Depositional Temperature of Quaternary Travertine Spring Mounds from Slovakia. *Minerals* **2023**, *13*, 794. https://doi.org/10.3390/min13060794

Academic Editors: Francesca Giustini and Mauro Brilli

Received: 5 April 2023
Revised: 1 June 2023
Accepted: 8 June 2023
Published: 10 June 2023

1. Introduction

The interest in travertine deposits as a paleoenvironmental and paleoclimatic tool has been well documented around the world. Recently, studies on travertines in Slovakia have compiled information on the forms, environments, facies, and ages of travertine sites [1,2], with a primary focus on the northern region of the country [3–5]. However, detailed information on the age, internal structure, and depositional environment is scarce in other regions of the country, where prior research has been limited to geothermal potential, hydrogeochemical, paleobotanical, and paleontological studies [6–10].

Situated in a tectonically complex area of the Western Carpathians and the northern edge of the Pannonian Basin, Slovakia has a favourable geological and tectonic structure for the occurrence of mineral and thermal waters in its territory, as well as several natural

travertine that form springs [1,2,11]. Some of the Slovakian springs present unique features, such as mounds and cones (e.g., Santovka, Dudince, Bojnice, Vyšné Ružbachy), and exhibit a rather low temperature of precipitation (e.g., Mičinské travertíny −8 °C) [12].

Spring mounds are spectacular forms of travertine deposits characterized by a circular topographic rise that develops around a spring vent. From the surface of a travertine mound, the water flows downward in depressed routes, precipitating calcium carbonate, calcite, and aragonite [13,14]. Travertine morphology is controlled by various factors, such as basement relief, potentiometric surface, CO_2 pressure, water chemistry, and temperature [4,14].

The potential preservation of physical, chemical, and microbial signatures, due to rapid precipitation, makes the travertine deposits valuable archives of environmental, geothermal, and geological processes that occur during periods of spring activity, in addition to allowing the identification of the temperature of carbonate-forming fluids, as well as the timing of precipitation [15–20]. In the present paper, we provide new stable isotope and radiometric age for active and inactive travertine mounds in Slovakia. The research focuses on the stable isotope geochemical study of these mounds, including the estimation of the deposition temperature and oxygen isotope composition of the travertine precipitating paleofluids using a carbonate-clumped isotope thermometry method.

2. Geological Settings

Slovakia (Figure 1A) is part of the Western Carpathians and was formed as a result of multiple tectonic processes involving the Variscan and Alpine tectogenesis [21,22]. The internal portion of the Western Carpathians is built by a nappe stack, which is represented by thick-skinned tectonic units (Gemericum, Veporicum, Tatricum) covered by a thin-skinned nappe system predominantly composed of Mesozoic variable carbonate rocks (Silicicum, Hronicum, Tatricum, Fatricum). Mineral springs are abundant in the country and are primarily associated with the Mesozoic carbonates and evaporites, as well as the Tertiary marine sediments. In several areas, travertine have been formed along deep faults, where some, such as the Variscan and Alpine faults, also provide escape routes for CO_2 [23].

The southern part of the territory is characterized by vast lowlands, extensions of the Neogene Pannonian Basin [24]. The travertine mounds located in this area (1—Santovka, 2—Dudince; Figure 1B) are situated on the Neogene volcanites that cover the nappe stacking formations of the Internal Western Carpathians. The basement of the volcanites is the Hronicum nappe near Santovka and the Veporicum tectonic units near Dudince. The Triassic part of these units consists mainly of limestone, which is the source of the dissolved carbonate content of the travertine-depositing mineral waters [8].

In the central region of Slovakia, the Čerín spring mounds (3, Figure 1B) rest directly on the Pliocene fluvial and the Holocene deluvial deposits in the Sliač-Hron region, which is part of the Neogene volcanites. The volcanic rocks lie on the deformed Mesozoic nappe system predominantly composed of Triassic limestone and dolomite of the Hronicum and Silicicum units [22]. Travertine springs at Liptovské Sliače (4), Bešeňová (5), and Liptovský Ján (6) (Figure 1B) were formed at different times and locations along tectonic faults in the Liptov Basin [25]. The basin is an intramountainous depression in the Internal Western Carpathians and is filled with Palaeogene sediments. The Mesozoic nappes, specifically the Triassic limestone and dolomite of the Hronicum unit and the Cretaceous limestone and marlstone of the Fatricum unit, form the basement of the Paleogene deposits and serve as sources for the dissolved carbonate content of mineral and thermal waters that feed the Liptov travertine springs [26].

The spring mounds located in northeastern Slovakia (7—Gánovce, 8—Vyšné Ružbachy, and 9—Sivá Brada; Figure 1B) are directly situated on the Holocene deluvial and fluvial deposits. The springs are recharged from limestone, dolomite, and evaporites of the Mesozoic nappe system. At Sivá Brada, the recharge source is derived from the Hronicum, Tatricum, and Veporicum units, while at Vyšné Ružbachy and Gánovce, it is acquired from the Fatricum and Hronicum units [27].

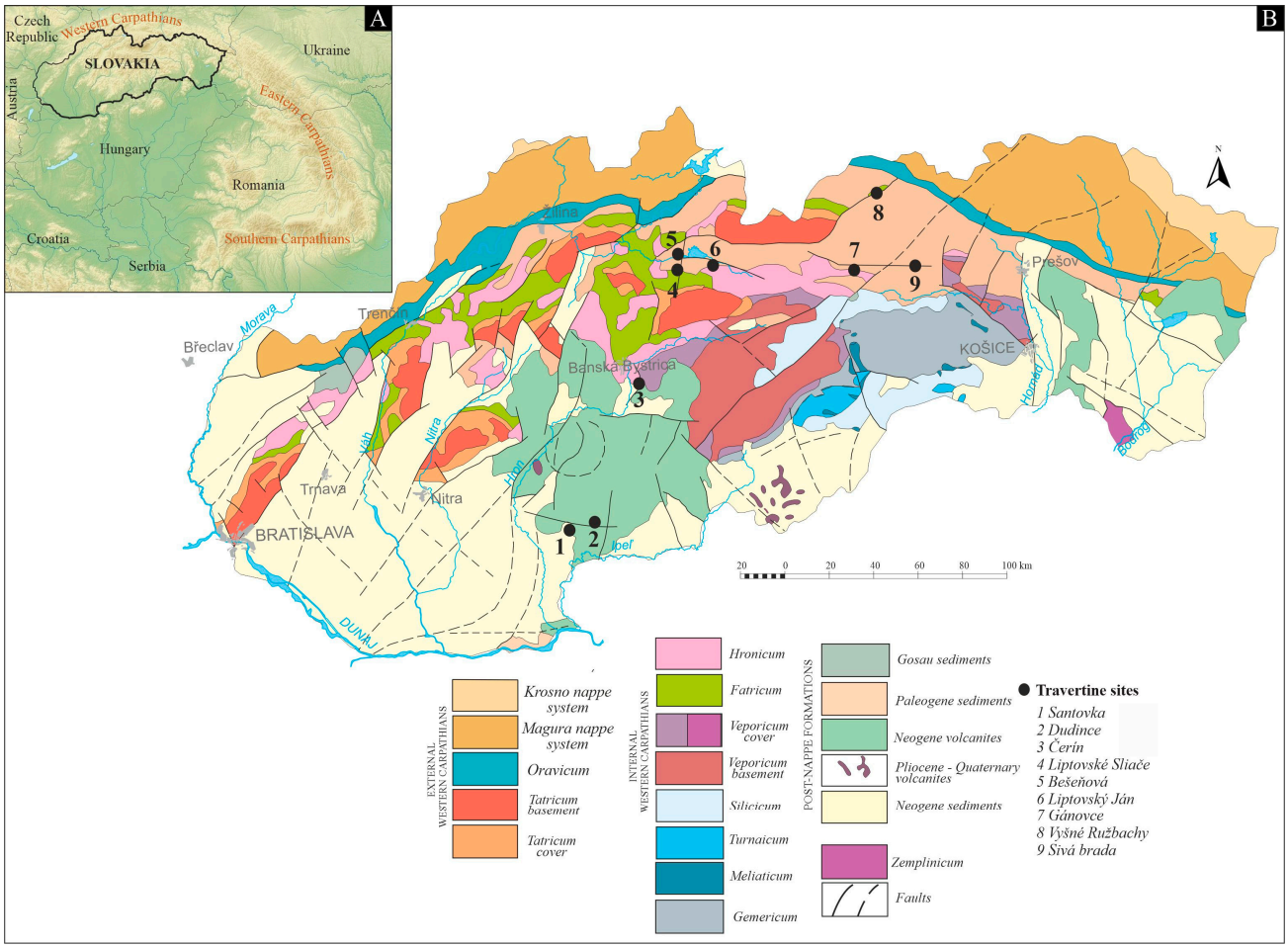

Figure 1. (**A**) Geographical setting of Slovakia and (**B**) tectonic sketch of Slovakia, modified from Hók et al. [26].

3. Materials and Methods

3.1. Field Studies and Sampling

The field research of this study was focused on active and inactive travertine spring mounds that occur at Santovka, Dudince, Čerin, Bešeňová, Liptovský Ján, Liptovské Sliače, Vyšné Ružbachy, Gánovce, and Sivá Brada (Figure 2). The sampling covered sections from the top to the base of each spring mound, starting with the vent and moving along the channels towards the distal parts downstream. In the case of active deposits, spring waters were also sampled at the vent and collected in 100 mL plastic bottles for stable isotope analyses. The basic physicochemical parameters of the water (pH, temperature) were measured in situ with a multi-parameter portable meter (WTW ProfiLine pH/Cond 3320).

Figure 2. Sampling sites in Slovakia. (**A**) Spring mound in Santovka Village; (**B**) Hostečný mound in Dudince spa; (**C**) Čerín spring mound (Mičinské travertíny); (**D**) Mound slopes with cascades in Bešeňová; (**E**) Kaď a natural crater in Liptovský Ján; (**F**) Vyšný Sliač crater; (**G**) Gánovce travertine spring; (**H**) Vyšné Ružbachy mound lake travertine; (**I**) Sivá Brada mound with recent orifices.

3.2. $\delta^{18}O$, $\delta^{13}C$, and $\delta^{2}H$ Analysis

The stable carbon and oxygen isotopic compositions ($\delta^{13}C$, $\delta^{18}O$) of the travertine samples and the oxygen and hydrogen isotopic compositions ($\delta^{18}O_w$, $\delta^{2}H$) of the water samples were performed using a Thermo Scientific Delta plus XP mass spectrometer (Thermo Scientific, Waltham, MA, USA) equipped with an automated GasBench II in the stable isotope laboratory of the Institute for Geological and Geochemical Research (IGGR), Research Centre for Astronomy and Earth Sciences (Budapest, Hungary). A total of samples were selected, powdered, and homogenized using an agate mortar and pestle, and stable carbon and oxygen isotope measurements were carried out on the bulk carbonate samples using the continuous flow technique with the H_3PO_4 digestion method [28]. The $\delta^{18}O$ values of the water samples ($\delta^{18}O_w$) were measured using the CO_2–water equilibration method [29]. The hydrogen isotope compositions were determined using the Pt-assisted H_2–H_2O equilibration [30].

Isotopic compositions of all the carbonate samples were measured in duplicate, and the water samples were measured in triplicate. The mean values are reported in the standard δ-notation in parts per thousand (‰) relative to Vienna PeeDee Belemnite (V-PDB; $\delta^{13}C$ and $\delta^{18}O$) and Vienna Standard Mean Ocean Water (V-SMOW; $\delta^{18}O_w$, $\delta^{2}H$). The reproducibility is better than ±0.1‰ for the $\delta^{13}C$ and $\delta^{18}O$ values of carbonates and ±0.1‰ and ±2‰ for $\delta^{18}O_w$ and $\delta^{2}H$, respectively. The accuracy was routinely verified by replicating the measurements of the laboratory standards calibrated to NBS19 and LSVEC.

3.3. Clumped Isotope Analysis

Clumped isotope analyses of the carbonates were carried out at the Isotope Climatology and Environmental Research Centre (ICER), Institute for Nuclear Research (ATOMKI), Debrecen. The analysis of the carbonate samples was performed on a Thermo Scientific 253 Plus 10 kV Isotope Ratio Mass Spectrometer after phosphoric acid digestion at 70 °C using a Thermo Scientific Kiel IV automatic carbonate device.

The negative background, which is caused by secondary electrons, was corrected by the application of the pressure-sensitive baseline correction [31] on all the raw beam signals. Approximately 100–120 µg aliquots of each carbonate sample measurement were replicated 11–12 times and measured alongside the carbonate standard samples. ETH1, ETH2, and ETH3 were used as normalization standards, and IAEA-C2 was used as a monitoring sample to determine the long-term reproducibility of the instrument. Simultaneously with the clumped isotope analysis, the conventional carbonate stable isotope composition was also determined for the same samples.

The data evaluation was carried out with Easotope software (release 20190125, concept by Cédric John, programmed by Devon Bowen) [32] using a CO_2-clumped ETH PBL replicate analysis method with the revised IUPAC parameters for ^{17}O correction [33–40]. The Δ_{47} results are given in the I-CDES90 scale [41], and the apparent temperatures in °C were calculated based on the Δ_{47}-temperature calibration from Anderson et al. [42] with one standard error.

3.4. U-Th Dating

The travertine samples were dated with the U-Th technique at the High–Precision Mass Spectrometry and Environmental Change Laboratory (HISPEC), Department of Geosciences, (National Taiwan University, Taipei, Taiwan) and at the Isotope Climatology and Environmental Research Centre (ICER), Institute for Nuclear Research (ATOMKI), Debrecen, Hungary. Both laboratories followed similar analytical procedures, where the selected samples were dissolved in a concentrated HNO_3 solution, and a triple spike (^{229}Th-^{233}U-^{236}U) was added. Later, 0.5 mL of $HClO_4$ was added to the sample solution to decompose the organic matter. Uranium and thorium final separation was achieved by a chemical method [43] and the protocol techniques for multi-collector inductively coupled plasma mass spectrometry [44] were used for determining the U-Th isotopic compositions and content.

Uncertainties in the U-Th isotopic data (corrections for blanks, multiplier dark noise, abundance sensitivity, contents of the four nuclides in a spike solution) were calculated at the 2σ level [43], and age corrections were calculated using an estimated atomic $^{230}Th/^{232}Th$ ratio of 4 (±2) × 10^{-6}. The half-lives of the U-Th nuclides used for age determination are reported by [45].

4. Results

4.1. U-Th Geochronological Data

The uranium and thorium isotopic compositions and the U-Th ages are summarized in Table 1 and Figure 3. The U-Th age data of this study cover a wide span between 301,072 ± 18,317 and 1156 ± 518 yr BP.

Table 1. U-Th dating results for travertine mounds in the study area.

Locality	^{238}U (ppb)	^{232}Th (ppt)	$\delta^{234}U$ [a]	$[^{230}Th/^{238}U]$ Activity [c]	$^{230}Th/^{232}Th$ (ppm)	Age (yr Ago) Uncorrected	Age (yr Ago) Corrected [c,d]	Age (yr BP) *	$\delta^{234}U_{initial}$ Corrected [b]
Santovka	71	3814 ± 8	1286 ± 5	0.1534 ± 0.0018	47 ± 1	7530 ± 91	6912 ± 323	6841 ± 323	1311 ± 5
	396	32,618 ± 3	471 ± 3	0.0856 ± 0.0005	19 ± 0	6515 ± 39	4880 ± 1157	4808 ± 1157	478 ± 4
	63	3190 ± 7	1027 ± 21	0.1400 ± 0.0020	46 ± 1	7759 ± 141	7104 ± 356	7032 ± 356	1048 ± 21
Dudince	139	52,503 ± 14	2518 ± 8	0.8431 ± 0.0017	37 ± 0	28,917 ± 95	25,925 ± 2124	25,853 ± 2124	2710 ± 18
	97	1335 ± 24	1213 ± 3	2.4304 ± 0.0403	2900 ± 71	301,239 ± 18,330	301,144 ± 18,317	301,072 ± 18,317	2838 ± 161
Lip. Sliače	370	15,187 ± 1	638 ± 4	0.0292 ± 0.0005	15 ± 0	1958 ± 35	1228 ± 518	1156 ± 518	640 ± 4
Lip. Ján	239	3686 ± 1	493 ± 3	0.1463 ± 0.0006	155 ± 1	11,188 ± 58	10,891 ± 218	10,819 ± 218	508 ± 4
Vyšné Ružbachy	789	20,995 ± 1	79 ± 2	0.9287 ± 0.0017	557 ± 1	204,146 ± 1871	203,465 ± 1919	203,393 ± 1919	140 ± 4
	806	835 ± 0	96 ± 2	0.1069 ± 0.0005	864 ± 13	11,174 ± 63	11,147 ± 66	11,075 ± 66	100 ± 3
	1320	130 ± 0	90 ± 2	0.1122 ± 0.0005	1806 ± 780	11,825 ± 65	11,827 ± 65	11,755 ± 65	93 ± 2
	978	8026 ± 2	106 ± 3	0.1006 ± 0.0007	193 ± 2	10,385 ± 80	10,169 ± 172	10,097 ± 172	109 ± 3
	1173	650 ± 0	89 ± 2	0.1060 ± 0.0005	1153 ± 26	11,149 ± 63	11,134 ± 64	11,062 ± 64	92 ± 2
Gánovce	163	1007 ± 0	448 ± 3	0.0979 ± 0.0005	240 ± 1	7612 ± 46	7489 ± 98	7417 ± 98	457 ± 3
	261	1207 ± 0	459 ± 3	0.0558 ± 0.0004	186 ± 2	4243 ± 34	4151 ± 73	4079 ± 73	465 ± 3

Analytical errors are 2σ of the mean. [a] $[^{238}U] = [^{235}U] \times 137{,}818$ (±0.65‰); $\delta^{234}U = ([^{234}U/^{238}U]_{activity} - 1) \times 1000$. [b] $\delta^{234}U_{initial}$ corrected was calculated based on ^{230}Th age (T), i.e., $\delta^{234}U_{initial} = \delta^{234}U_{measured} \times e^{l234xT}$ and T is corrected age. [c] $[^{230}Th/^{238}U]activity = 1 - e^{-l230T} + (\delta^{234}U_{measured}/1000)[\lambda_{230}/(\lambda_{230} - \lambda_{234})](1 - e^{-(\lambda 230 - \lambda 234)T})$, where T is the age. Decay constants are 9.1705 × 10^{-6} yr^{-1} for ^{230}Th, 2.8221 × 10^{-6} yr^{-1} for ^{234}U, and 1.55125 × 10^{-10} yr^{-1} for ^{238}U. [d] Age corrections, relative to chemistry date on 4 October 2021, were calculated using an estimated atomic $^{230}Th/^{232}Th$ ratio of 4(±2) ppm. Those are the values for a material at secular equilibrium with a crustal $^{232}Th/^{238}U$ value of 3.8. The errors are arbitrarily assumed to be 50%. * BP stands for "Before Present", where the "Present" is defined as the year 1950 A.D.

The oldest travertine (301,072 ± 18,317 yr BP), the Tatar Spring (Tatársky prameň) at Dudince, is characterized by a semi-spherical spring mound with a diameter of 860 m and a height of about 8 m, and a crater on top (Figure 3B). At Dudince, a younger age of 25,853 ± 2124 yr BP was also obtained for the largest travertine terrace with a height of approximately 5 m. The terrain was formed by several mounds joined together, and this age refers to the top of the crater of the original spring, preserved on the highest flat spring mound (Figure 3C).

Figure 3. Sampled points for U-Th dating and obtained ages (±2σ) at the studied sites. Ages are reported in years before present (yr BP). (**A**) Spring mound in Santovka Village; (**B**) Tatarsky spring mound at Dudince; (**C**) Rímske Kúpele mound at Dudince; (**D**) Vyšný Sliač spring mound crater; (**E**) "White house" inactive travertine crater in Vyšné Ružbachy; (**F**) Vyšné Ružbachy crater-like orifice and small spring mound downstream; (**G**) Gánovce travertine mound; (**H**) Inactive travertine mound in Liptovský Ján.

At Vyšné Ružbachy, two generations of travertine deposits are recognized. The oldest sample at Vyšné Ružbachy (Figure 3F) is an old crater with a depth of 3.5 m, which is currently filled with water at a temperature of about 22 °C. The age determination of this sample yields an age of 203,393 ± 1919 yr BP. The youngest travertine generation is represented by a small travertine mound 3 m from the crater (Figure 3F) with an age of 11,075 ± 66 yr BP and the "White House" inactive crater (Figure 3E), with ages of 11,755 ± 65, 11,062 ± 64 and 10,097 ± 172 yr BP, obtained from the base, middle, and top, respectively. An inactive mound at Liptovský Ján (Figure 3H) shows a similar age of 10,819 ± 218 yr BP.

At Santovka, a large mound 5 m high and 40 m in diameter, and a small crater at the top (Figure 3A) were also sampled from the base to the top, yielding ages of 7032 ± 356, 6841 ± 323, and 4808 ± 1157 yr BP, respectively. Similarly, younger ages were obtained from the youngest part of the Gánovce mound (7417 ± 98 and 4079 ± 73 yr BP, Figure 3G). In Liptovské Sliače, an inactive broad orifice and two small craters of different sizes were found, but only the small one (Figure 3D) was successfully dated, providing the youngest age of 1156 ± 518 yr BP.

4.2. Isotopic Composition of Carbonates ($\delta^{18}O$, $\delta^{13}C$, and Δ_{47})

The carbon and oxygen isotope compositions of all the travertine samples are reported in Table S1 (see the supplementary materials) and displayed in Figure 4. The results show positive $\delta^{13}C$ values for all the sites, ranging from 4.9 to 12.3 (‰, V-PDB). The $\delta^{18}O$ values (V-PDB) are negative and range between −12.2 and −5.8 (‰, V-PDB).

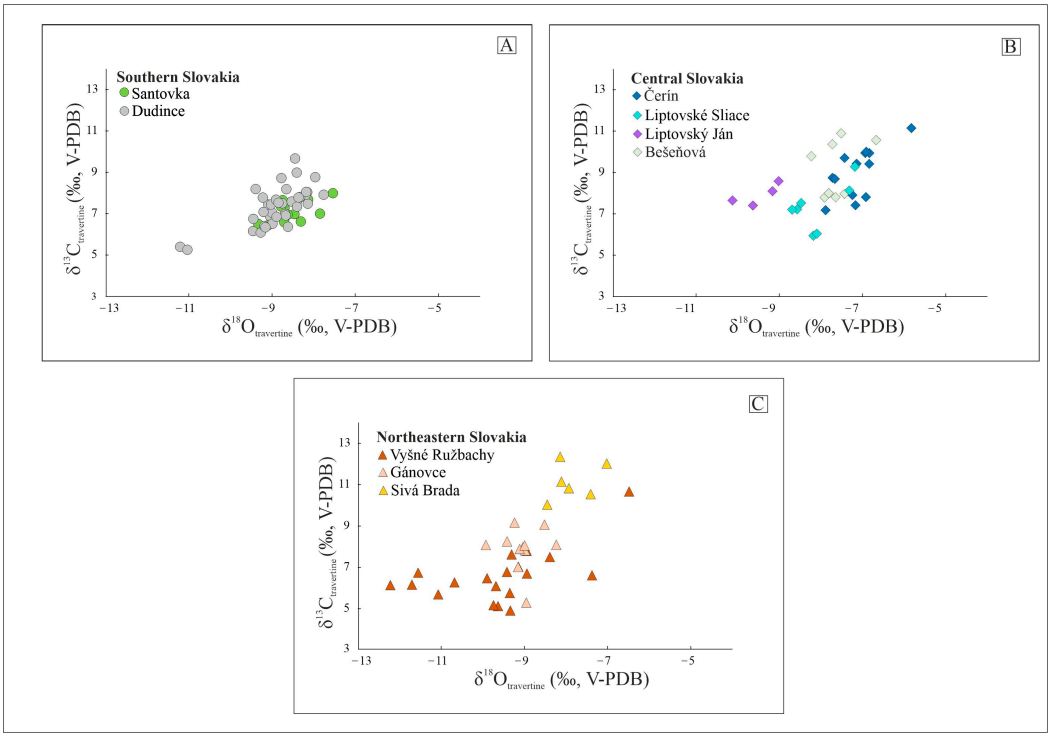

Figure 4. Stable isotope composition of the Slovakian travertine spring mounds (See Table S1) of (**A**) Southern Slovakia, (**B**) Central Slovakia and (**C**) Northeastern Slovakia.

The clumped isotope composition (Δ_{47}) of the inactive travertine mounds was measured in the samples collected from the orifices (presenting close to equilibrium conditions, as suggested by Kele et al. [46]) and from the base of each selected mound to reconstruct the palaeotemperature of the depositing fluids. The $\Delta_{47(I\text{-}CEES90)}$ values range from 0.571 to 0.668‰, whereas the calculated deposition temperatures varied between 10 and 32 °C,

4 and 18 °C, and 17 and 21 °C for southern, central, and northeast Slovakia, respectively (Table 2 and Table S3).

Table 2. Clumped isotope results and calculated $\delta^{18}O_w$.

Locality	ID	Lithofacies	$\delta^{13}C$ (V-PDB) ‰	$\delta^{18}O$ (V-PDB) ‰	Δ_{47} (I-CDES90) (‰)	Δ_{47} (I-CDES90) std Error (‰)	$T\Delta_{47}$ (°C)	±	$\delta^{18}O_w$	$\delta^{13}C_{CO2}$	T °C
1	STV5	Vent	6.4	−9.0	0.571	0.0111	32	4	−8.1	−2.9	11.2–26 *
	STV38	Distal Slope	7.2	−8.6	0.638	0.0089	10	3	−12.7	−1.9	
2	DUD1	Vent	7.7	−8.2	0.608	0.0148	20	5	−10.0	−1.3	10.7–30 *
	DUD2	Vent	7.8	−8.0	0.604	0.0089	21	3	−9.6	−1.1	
	DUD6	Proximal Slope	7.9	−8.2	0.601	0.0148	22	5	−9.5	−1.0	
	DUD15	Distal Slope	8.0	−8.1	0.614	0.0070	18	2	−10.3	−0.9	
	DUD18	Vent	8.0	−8.4	0.588	0.0120	26	4	−8.8	−0.9	
	DUD23	Vent	7.6	−8.9	0.631	0.0103	12	3	−12.5	−1.4	
	DUD29	Parasite Vent	8.3	−8.8	0.582	0.0100	28	4	−8.7	−0.6	
3	C7	Vent	7.5	−7.3	0.660	0.0104	4	3	−13.0	−1.5	7.9–13.3
4	S14	Vent	6.5	−7.8	0.655	0.0140	6	4	−13.0	−2.8	17.4
	S19	Distal Slope	7.5	−8.6	0.613	0.0136	18	4	−10.8	−1.5	
5	L24	Distal Slope	8.4	−9.1	0.650	0.0124	7	3	−13.9	−0.5	18.7–24.5
6	B32	Proximal Slope	7.2	−7.3	0.652	0.0070	6	2	−12.4	−1.8	14–15.6
	B34	Distal Slope	7.8	−8.0	0.632	0.0063	12	2	−11.6	−1.2	
7	N12	Distal Slope	6.5	−10.1	0.604	0.0099	21	3	−11.6	−2.7	20.7–22.2
	N13	Proximal Slope	6.2	−12.1	0.609	0.0115	19	4	−14.0	−3.0	
8	N27	Distal Slope	8.0	−8.9	0.615	0.0104	17	3	−11.4	−0.9	22.4–23.8
	N29	Distal Slope	9.2	−9.3	0.618	0.0108	17	3	−11.7	0.5	
9	N32	Vent	10.1	−8.5	0.608	0.0162	20	5	−10.2	1.7	5.5–13.6

1. Santovka, 2. Dudince, 3. Čerín, 4. Liptovské Sliače, 5. Liptovský Ján, 6. Bešeňová, 7. Vyšné Ružbachy, 8. Gánovce, 9. Sivá brada. Δ_{47}-based temperature ($T\Delta_{47}$) was calculated using the equation presented by Anderson et al. [42]. $\delta^{18}O_w$ was calculated using the equation of Kele et al. [46]. $\delta^{13}C_{CO2}$ was calculated using the empirical equation of Panichi and Tongiorgi [47]. T°C is temperatures measured nowadays. * Data taken from Bačová et al. [48].

4.3. Isotopic Composition of Water ($\delta^{18}O_w$, δ^2H)

The stable hydrogen and oxygen isotope composition of the water sampled at active travertine spring mounds, together with the measured physicochemical parameters are reported in Table S2. The δ^2H values of the water are quite high, ranging between −80.5‰ and −58.3‰ (V-SMOW), whereas the $\delta^{18}O_w$ values vary from −11.4‰ to −8.9‰ (V-SMOW). When plotted in the $\delta^2H/\delta^{18}O_w$ diagram (Figure 5), they fall along the trend defined by local (LMWL) [49] and global (GMWL) [50] meteoric water lines.

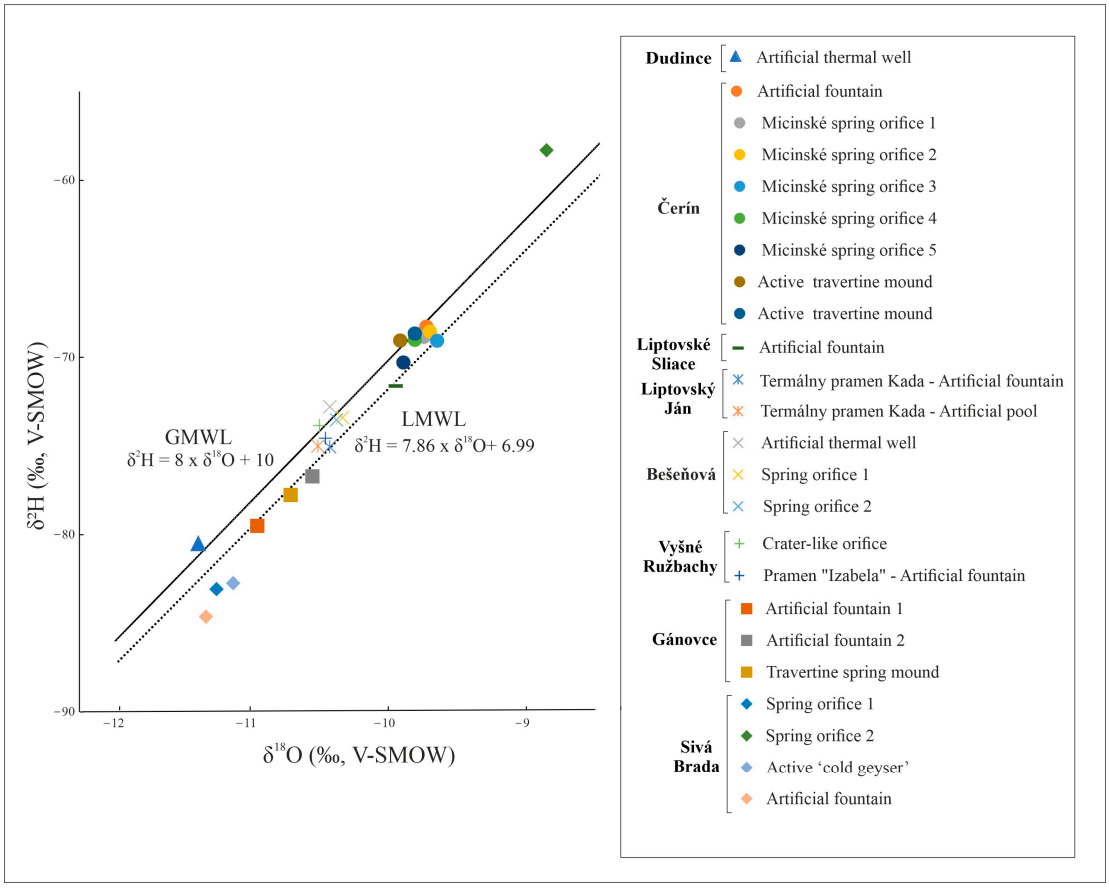

Figure 5. Isotopic compositions of water samples of travertine-forming springs in Slovakia, indicating the global (GMWL) and local meteoric line (LMWL) for comparison.

5. Discussion

5.1. U-Th Ages

Several travertine occurrences can be found in Slovakia [1], which are often formed on fault intersections and are related to extensional tectonics. Detailed data about their age are very limited and thus far, the time of their deposition has mainly been assumed based on paleobotanical, malacological, and paleontological finds and geomorphological data [26,51–60]. The U-Th data were only published by Kovanda et al. [61] for the Skalka travertine mound, and Gradziński et al. [3] for sites located at Vyšné Ružbachy, Lúčky, and Bešeňová. Pivko and Vojtko [1] summarized the published age data of Slovakian travertine.

The geochronological data of travertine can provide information about the paleoclimate of continental environments since travertine deposition is commonly linked with warm and wet climate conditions during the Quaternary period [11,62–64]. Changes in climatic conditions, including cold (glacial) and warm (interglacial) periods, can impact the development of mineral and thermal waters. To investigate the possible relationship between travertine deposition and the paleoclimate in the study area, Figure 6 presents the $\delta^{18}O$ isotope stack record [65] and indicates the ages of the studied travertine. These data show that Slovakian travertine precipitated in both glacial and interglacial periods, with a tendency towards warmer climate conditions. The samples were dated to the MIS 1, 2, 7, and 9 periods. It is important to note that the MIS 9 sample has a relatively high error margin, which suggests that it could potentially extend partially into MIS 8.

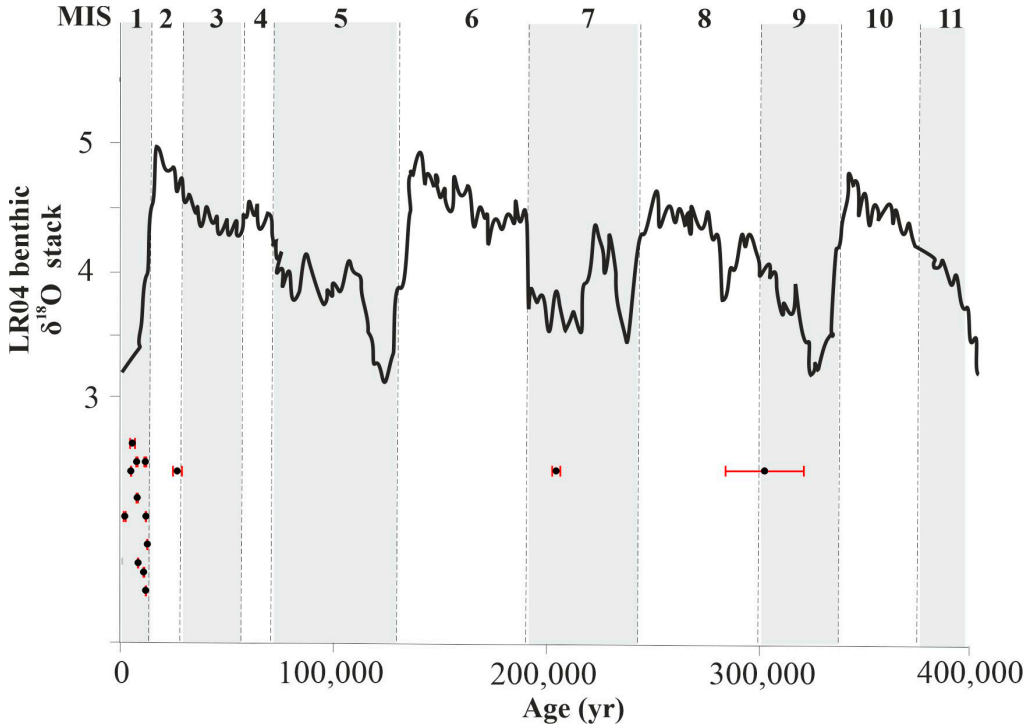

Figure 6. U-Th ages of Slovakian travertine compared with LR04 benthic isotope stack record (Lisiecki and Raymo [65]). Dated samples (black circle) display error bars in red. Global glacial periods (white bars) and interglacial periods (shaded bars) are shown by marine isotope stages (MIS) defined by Lisiecki and Raymo [65].

Although our geochronological data are in agreement with previous studies in Slovakia, suggesting deposition during warm and humid periods of the Holocene [66], the correlation with climate phases seems uncertain, as shown by travertine ages that fit MIS 2 (glacial) and MIS 8/9 (glacial/interglacial) periods.

Dudince (301,072 ± 18,317 yr BP) and Vyšné Ružbachy (203,393 ± 1919 yr BP) appear to be correlated with interglacial stages (Figure 6) in the Pleistocene. However, the Dudince site also shows a U-Th age of 25,853 ± 2124, suggesting another deposition in MIS 2 during the last glacial maximum (LGM) (26.5–19 ka) [67]. The correspondence between the travertine ages and glacial/interglacial times suggests that travertine deposition was not completely absent during glacial periods, but likely reduced [68].

Travertine deposition during dry glacial periods can indicate tectonic activity, rather than climate influence, since faults control the movement of CO_2-rich water toward the surface [69,70]. Deeply derived CO_2 is expected to be present during both glacial and interglacial periods, and fluid recharge related to global and regional climate would provide the necessary water for the observed travertine deposition in dry periods. In Slovakia, the distribution of mineral water is closely related to well-known deep faults and geological structures in the country [23], which facilitate long-distance communication between carbon dioxide sources and mineral water collectors.

The Holocene is well documented by our age data measured from the travertine deposits of Santovka, Liptovský Ján, Liptovské Sliače, Vyšné Ružbachy, and Gánovce with a time interval between 1156 ± 518 and 11,755 ± 65 yr BP, reflecting a time of a warm and wet climate [64,66]. During this period, the recharge of a groundwater aquifer could have been increased and travertine deposition occurred during glacial terminations and continued into interglacial times.

5.2. Travertine Classification and Isotope Signature

The $\delta^{13}C$ values are used to geochemically classify the travertine deposits into two main groups [71]. Thermogene travertine show $\delta^{13}C$ values between −3‰ and +10‰, while meteogene travertine are characterized by lower $\delta^{13}C$ values between −12‰ and +2‰ [14]. The $\delta^{13}C$ data of the studied Slovakian travertine (+4.9 to +12.3‰, V-PDB) show a typical thermogene isotope value similar to the ones found in previous studies for travertine in Slovakia [3,5], Italy [72–74], and Turkey [75,76].

The positive $\delta^{13}C$ and negative $\delta^{18}O$ values obtained for all the samples analyzed suggest a combination of hydrothermal fluids and meteoric water with a contribution of heavy CO_2 formed by the thermal decomposition of carbonate rocks at depth [75]. The $\delta^{13}C$ values observed in the active travertine deposits at Čerin, Bešeňová, Vyšné Ružbachy, and Sivá brada are more positive than +10‰ (Table S1). The shift in the $\delta^{13}C$ values up to +11.7‰ V-PDB are thought to be a result of more rapid CO_2-degassing, which is associated with fast flowing water on the steeper parts of the downslope [75,76]. In the case of the vent samples of active springs, the shift can be attributed to the presence of bacterial mats, since these organisms can locally remove isotopically light CO_2 [75].

The $\delta^{13}C$ data of travertine can be used to determine the source of carbon dioxide once the $\delta^{13}C$ value of the travertine is controlled by the carbon species dissolved in the groundwater. Based on that, the $\delta^{13}C$ of the CO_2 was calculated using the equation $\delta^{13}C_{(CO2)} = 1.2(\delta^{13}C_{(Trav)}) - 10.5$ proposed by Panichi and Tongiorgi [47], to calculate the original $^{13}C/^{12}C$ ratios of CO_2 from the $\delta^{13}C$ values measured in the fossil travertine. These calculated values correspond to the $\delta^{13}C$ of the CO_2 released from the water during travertine deposition [17,77]. The calculated $\delta^{13}C_{CO2}$ of our samples (Table 2) range from −3 to 1.7‰.

Generally, the $\delta^{13}C$ values of CO_2 originating from magmatic sources show values from −7 to −5‰ [78] and measurements of the $^{3}He/^{4}He$ ratios confirmed the presence of mantle-derived gas in the Carpathian Basin [79–81]. However, the $\delta^{13}C$ values calculated from the measured travertine values are more positive (−3 to 1.7‰) than the $\delta^{13}C$ value of CO_2 coming from a pure igneous source, which suggests a mixed origin.

Cornides and Kecskés [79] examined CO_2 discharges in Slovakia, obtaining $\delta^{13}C$ values in the range of −6 to −3‰, indicating the presence of CO_2 of a mantle origin. Despite this, the final stable carbon isotope composition of travertine can be influenced by the carbon dissolved from the primary carbonate rock. Since in the Carpathian Basin the carbonates in the bedrock show $\delta^{13}C$ values in a range of 0 to 3‰ [79], the positive values calculated for the Slovakian travertine (Table S3) could derive from isotopically heavy CO_2 liberated during thermometamorphic decarbonation of carbonate basement rocks, such as Triassic limestone from Silicicum, Hronicum, Tatricum, and Fatricum units.

5.3. Paleotemperatures

The temperature of the fluid was determined using clumped isotope thermometry and shows variations across different sites. The comparison with the temperature of the modern fluids measured in situ at active springs (5.5 to 26.9 °C) is shown in Table 2.

In southern Slovakia, the Santovka clumped isotope paleotemperatures were found to be 32 ± 4 °C at the vent and 10 ± 3 °C for a sample collected from a distant slope of the mound. Bačová et al. [48] obtained a temperature range of 11.2 to 26 °C measured in situ, which is similar to our calculated paleotemperatures (Table 2). At the Dudince site, three different vent samples showed paleotemperatures of 21 ± 3, 12 ± 3, and 28 ± 4 °C. The temperatures of 12 ± 3 and 28 ± 4 °C were calculated from samples collected from the same mound, but the higher temperature was obtained from a sample collected from a younger parasite vent located on the slope of the mound. The current temperature measurements at the site range between 10.7 °C and 30 °C [48], indicating no significant difference from the paleotemperatures. The colder temperature (12 ± 3 °C) could indicate a mixture with cold precipitation or the formation of a pool at the top of the vent.

In central Slovakia, the Čerín clumped isotope paleotemperature was found to be 4 ± 3 °C, which is consistent with the current temperatures within the range of error. At Vyšný Sliač, a sample collected from a broad orifice of approximately 25 m in diameter showed a paleotemperature of 6 ± 4 °C, while a sample collected from the distal part of a different mound showed a temperature of 18 ± 4 °C, similar to the temperature of 17.4 °C measured at an artificial fountain on the slope of this mound. The paleotemperature of 6 ± 4 °C was collected on the edge of the 25 m diameter orifice. Considering that water temperature tends to decrease as the distance from the spring orifice increases, this sample may be located at a considerable distance from the actual spring orifice. Here, kinetic effects, such as fractionation resulting from water evaporation and CO_2 degassing, may have influenced the isotope data. These effects could have led to an enrichment of ^{18}O in the calcite, lowering the calculated temperature.

The same case is applied to the Bešeňová and Liptovský Ján data. At Bešeňová, paleotemperatures were calculated from samples collected at the top (6 ± 2 °C) and base (12 ± 2 °C) of the so-called "Rock tower" travertine, which is approximately 9 m high, and consists of a layered deposit. Close to this site, the present spring water temperature ranges between 14 °C and 15.6 °C. At Liptovský Ján, the clumped isotope paleotemperature calculated for a sample collected at the distal slope of an inactive mound was 7 ± 3 °C, while the current water temperature measurements range from 18.7 °C to 24.5 °C. Since the exact location of the vent could not be identified, it is not possible to make a reliable comparison with the measured temperatures.

In northeastern Slovakia, paleotemperatures were determined at Vyšné Ružbachy, with results of 19 ± 4 °C and 21 ± 3 °C. These values are comparable to recent temperature measurements at the site, which range from 20.7 °C to 22.2 °C. At Gánovce, the paleotemperature found was 17 ± 3 °C, which is similar to the current temperature range of 22.4 °C to 23.8 °C, when considering the error (±3). Sivá Brada exhibited paleotemperatures of 20 ± 5 °C for vent samples, which are significantly higher than the current temperatures of 5.5–13.6 °C. These differences in temperature could be attributed to several factors, such as changes in the hydrothermal system, mixing with cooler surface waters, or variations in the thermal input. Further detailed studies of each site would be needed to determine the exact cause of the temperature discrepancy.

5.4. Isotopic Signature of Paleofluids

The isotopic composition of water provides useful information about its origin, mixing between different sources, and water–rock interaction processes [82]. The $\delta^{18}O_w$ values were plotted against the δ^2H values for the study area (Figure 5) and have been compared to the global meteoric water line (GMWL) [50] and the local meteoric water line (LMWL), with the latter defined by the equation $\delta^2H = 7.86 \times \delta^{18}O + 6.99$ [49]. The LMWL is considered more accurate than the GMWL given the climatic/topographic conditions of the study area.

The meteoric origin of spring water is strongly suggested by the linear distribution of δ^2H and $\delta^{18}O_w$ along the GMWL and LMWL lines (as shown in Figure 5). The values of the mineral waters fall along the lines, with the lower part reflecting colder climate conditions during the infiltration processes [83]. One water sample from the Sivá Brada site ($\delta^{18}O_w$: −8.9, δ^2H: −58.3) displays the highest stable isotope composition and lies slightly above the GMWL. This could indicate a warmer climate during infiltration and mixing with young, fresh water.

We calculated the $\delta^{18}O_w$ of the travertine precipitating fluid (Table 2) from the measured carbonate $\delta^{18}O$ values and the $T_{\Delta 47}$ values using the equation of Kele et al. [46]. This empirical equation is expressed as $1000\ln\alpha_{\text{(calcite-water)}} = (20 \pm 2)\ 1000/T - (36 \pm 7)$, where α (calcite-water) = $(\alpha^{18}O_{calcite} + 1000)/(\alpha^{18}O_{water} + 1000)$ and T is the temperature of the mineralizing $CaCO_3$-rich fluids ($T_{\Delta 47}$) expressed in K.

These data indicate that the aquifer water forming the travertine deposits could have had $\delta^{18}O_w$ values between −14 and −8.1‰. The water of the modern springs has an

isotope composition range of −80.5‰ to −58.3‰ (V-SMOW) and −11.4‰ to −8.9‰ (V-SMOW) for δ^2H and $\delta^{18}O_w$, respectively. This $\delta^{18}O$ variability between past and recent values could be interpreted as an influence of present-day precipitation (−10.4‰ to −8.7‰) on the water in this region [84].

6. Conclusions

This study investigated travertine mound springs of different regions of Slovakia through water and carbonates isotope geochemistry, clumped isotope, and U-Th geochronology. Integration of these new data permitted us to outline the general features of paleofluid circulation in this region and the deposition age of these travertine.

Based on their positive $\delta^{13}C$ values, the travertine samples are of thermogene origin. The deposition temperatures estimated from clumped isotope analysis (Δ_{47}) range from 4 ± 3 to 32 ± 4 °C, characteristic of cold to warm springs. The clumped isotope paleotemperature data obtained for Slovakian travertine have provided valuable insights into the past temperature trends of paleospring systems in the region. The similarities observed between paleo and current temperatures suggest that the paleospring systems have not change significatively over the time, but have remained relatively stable. In the case of Sivá Brada, the discrepancy in temperatures could be attributed to several factors (changes in the hydrothermal system, mixing with cooler surface waters, or variations in the thermal input), and more research is needed to better understand these variations.

Slovakian travertine mounds may have formed due to the deposition of meteoric-derived fluids, which were able to rise upwards along basement-penetrating faults. The travertine depositional age provided by the U-Th method varies in a wide range from 1.2 to 301 ka and demonstrates that it has been deposited mostly in warm and wet periods, but also in cold and dry periods.

Our results can contribute to the knowledge of the formation of the mineral water and travertine in Slovakia and could serve as a base for further detailed geochronological and geochemical studies to reconstruct the paleoclimate and paleoenvironment during their deposition.

Supplementary Materials: The following supporting information can be downloaded at: https://www.mdpi.com/article/10.3390/min13060794/s1, Table S1: Stable isotope composition of the Slovakia travertine spring mounds. Table S2: Temperature, pH and stable isotope composition of the water samples. $\delta^{18}O$ and δ^2H values are expressed in the δ notation (‰) against V-SMOW. * Data taken from Franko et al. [84]. Table S3: Complete clumped isotope results and calculated $\delta^{18}O_w$. Table S4: Travertine locations with GPS coordinates and brief description of each site.

Author Contributions: D.S.C.V. wrote the manuscript and prepared the figures and tables. D.S.C.V., S.K. and D.P. performed field work. S.K. supervised the research. L.R. performed clumped isotope analysis of carbonate. D.S.C.V., L.P. and G.I.K. performed U-series analysis at ATOMKI. H.-M.H. and C.-C.S. performed U-series analysis at HISPEC. All authors have read and agreed to the published version of the manuscript.

Funding: This research was funded by the European Union and the State of Hungary and co-financed by the European Regional Development Fund in the project of GINOP-2.3.2-15-2016-00009 'ICER'. This research was also supported by Tempus Public Foundation, Stipendium Hungaricum Scholarship and the Doctoral School of Earth Sciences at Eötvös Loránd University (ELTE).

Data Availability Statement: All data are available in the article.

Acknowledgments: We kindly thank the anonymous reviewers for their valuable comments, which have significantly improved the quality of the manuscript.

Conflicts of Interest: The authors declare no conflict of interest.

References

1. Pivko, D.; Vojtko, R. A review of travertines and tufas in Slovakia: Geomorphology, environments, tectonic pattern, and age distribution. *Acta Geol. Slovaca* **2021**, *13*, 49–78.
2. Pivko, D. A review of Slovak travertine and tufa facies and their environment. *Acta Geol. Slovaca* **2021**, *13*, 129–166.
3. Gradziński, M.; Dulinski, M.; Hercman, H.; Stworzewicz, E.; Holúbek, P.; Rajnoga, P.; Wroblewski, W.; Kováčová, M. Facies and age of travertines from Spiš and Liptov regions (Slovakia)—Preliminary results. *Slov. Kras (Acta Carsologica Slovaca)* **2008**, *46*, 31–40.
4. Gradziński, M.; Wroblewski, W.; Bella, P. Cenozoic freshwater carbonates of the Central Carpathians (Slovakia): Facies, environments, hydrological control and depositional history. In *Guidebook Field Trips Accompanying, Proceedings of the 31st IAS Meeting of Sedimentology, Kraków, Poland, 22–25 June 2015*; Polish Geological Society: Kraków, Poland, 2015; pp. 217–245.
5. Gradziński, M.; Wróblewski, W.; Duliński, M.; Hercman, H. Earthquake-affected development of a travertine ridge. *Sedimentology* **2014**, *61*, 238–263. [CrossRef]
6. Kriš, J.; Marton, J.; Skultétyová, I. Mineral and geothermal waters of Slovakia. *GeoJournal* **1995**, *35*, 431–442. [CrossRef]
7. Hyánková, K.; Melioris, L. The unusual chemism of mineral waters at Dudince. *Geol. Carpathica* **1993**, *44*, 123–131.
8. Melioris, L. Mineral and thermal waters of the Ipelská Pahorkatina hillyland. *Environ. Geol.* **2000**, *39*, 448–462. [CrossRef]
9. Šolcová, A.; Petr, L.; Hájková, P.; Petřík, J.; Tóth, P.; Rohovec, J.; Bátora, J.; Horsák, M. Early and middle Holocene ecosystem changes at the Western Carpathian/Pannonian border driven by climate and Neolithic impact. *Boreas* **2018**, *47*, 897–909. [CrossRef]
10. Dabkowski, J.; Frodlová, J.; Hájek, M.; Hájková, P.; Petr, L.; Fiorillo, D.; Dudová, L.; Horsák, M. A complete Holocene climate and environment record for the Western Carpathians (Slovakia) derived from a tufa deposit. *Holocene* **2019**, *29*, 493–504. [CrossRef]
11. Pentecost, A. Geochemistry of carbon dioxide in six travertine-depositing waters of Italy. *J. Hydrol.* **1995**, *167*, 263–278. [CrossRef]
12. Scheuer, G.; Schweitzer, F. A Kárpát-Medence környéki édesvizi mészköelöfordulások összehasonlitésa a hazai adottságokkal, I. Szlovákia. *Földtani Közlöny* **1981**, *111*, 453–471.
13. Chafetz, H.S.; Folk, R.L. Travertines; depositional morphology and the bacterially constructed constituents. *J. Sediment. Res.* **1984**, *54*, 289–316. [CrossRef]
14. Pentecost, A. *Travertine*; Springer Science & Business Media: Berlin/Heidelberg, Germany, 2005.
15. Fouke, B.W.; Farmer, J.D.; Des Marais, D.J.; Pratt, L.; Sturchio, N.C.; Burns, P.C.; Discipulo, M.K. Depositional Facies and Aqueous-Solid Geochemistry of Travertine-Depositing Hot Springs (Angel Terrace, Mammoth Hot Springs, Yellowstone National Park, U.S.A.). *J. Sediment. Res.* **2000**, *70*, 565–585. [CrossRef] [PubMed]
16. Andrews, J.E.; Riding, R.; Dennis, P.F. The stable isotope record of environmental and climatic signals in modern terrestrial microbial carbonates from Europe. *Palaeogeogr. Palaeoclimatol. Palaeoecol.* **1997**, *129*, 171–189. [CrossRef]
17. Minissale, A.; Kerrick, D.M.; Magro, G.; Murrell, M.T.; Paladini, M.; Rihs, S.; Sturchio, N.C.; Tassi, F.; Vaselli, O. Geochemistry of Quaternary travertines in the region north of Rome (Italy): Structural, hydrologic and paleoclimatic implications. *Earth Planet. Sci. Lett.* **2002**, *203*, 709–728. [CrossRef]
18. Liu, Z.; Zhang, M.; Li, Q.; You, S. Hydrochemical and isotope characteristics of spring water and travertine in the Baishuitai area (SW China) and their meaning for paleoenvironmental reconstruction. *Environ. Geol.* **2003**, *44*, 698–704. [CrossRef]
19. Kano, A.; Okumura, T.; Shiraishi, F.; Takashima, C. *Geomicrobiological Properties and Processes of Travertine: With a Focus on Japanese Sites*, 1st ed.; Springer: Singapore, 2019; p. 181.
20. Brogi, A.; Capezzuoli, E.; Moretti, M.; Olvera-García, E.; Matera, P.F.; Garduno-Monroy, V.-H.; Mancini, A. Earthquake-triggered soft-sediment deformation structures (seismites) in travertine deposits. *Tectonophysics* **2018**, *745*, 349–365. [CrossRef]
21. Bezák, V.; Biely, A.; Elečko, M.; Konečný, V.; Mello, J.; Polák, M.; Potfaj, M. A new synthesis of the geological structure of Slovakia—The general geological map at 1:200,000 scale. *Geol. Q.* **2011**, *55*, 1–8.
22. Hók, J.; Pelech, O.; Teťák, F.; Németh, Z.; Nagy, A. Outline of the geology of Slovakia (W. Carpathians). *Miner. Slovaca* **2019**, *51*, 31–60.
23. Franko, O.; Franko, J. Thermal waters of the Hornonitrianska kotlina depression and their utilization. *Environ. Geol.* **2000**, *39*, 501–515. [CrossRef]
24. Bodiš, D.; Remšík, A.; Černák, R.; Marcin, D.; Ženišová, Z.; Fl'aková, R. Geothermal and hydrogeological conditions, geochemical properties and uses of geothermal waters of the Slovakia. In *Geothermal Water Management, 1 ed.*; Bundschuh, J., Tomaszewska, B., Eds.; CRC Press: Boca Raton, FL, USA, 2018; pp. 41–62.
25. Chrobak-Žuffová, A.; Papčo, P. Liptov region and its geotourism wealth. In Proceedings of the GEOTOUR & IRSE 2014, Miskolc, Hungary, 16–18 October 2014; pp. 98–108.
26. Hók, J.; Kováč, M.; Rakús, M.; Kováč, P.; Nagy, A.; Kováčová-Slamková, M.; Sitár, V.; Šujan, M. Geologic and tectonic evolution of the Turiec depression in the Neogene. *Slovak Geol. Mag.* **1998**, *4*, 165–176.
27. Michalko, J.; Fendek, M. Environmental isotopes in groundwaters of Levočskê Kotlina Basin. In Proceedings of the XVII Congress of Carpathian-Balkan Geological Association, Bratislava, Slovakia, 1–4 September 2002.
28. Spötl, C.; Vennemann, T.W. Continuous-flow isotope ratio mass spectrometric analysis of carbonate minerals: Letter to the Editor. *Rapid Commun. Mass Spectrom.* **2003**, *17*, 1004–1006. [CrossRef]

29. Epstein, S.; Mayeda, T. Variation of O^{18} content of waters from natural sources. *Geochim. Cosmochim. Acta* **1953**, *4*, 213–224. [CrossRef]
30. Coplen, T.B.; Wildman, J.D.; Chen, J. Improvements in the gaseous hydrogen-water equilibration technique for hydrogen isotope-ratio analysis. *Anal. Chem.* **1991**, *63*, 910–912. [CrossRef]
31. Bernasconi, S.M.; Hu, B.; Wacker, U.; Fiebig, J.; Breitenbach, S.F.M.; Rutz, T. Background effects on Faraday collectors in gas-source mass spectrometry and implications for clumped isotope measurements: Background effects on Faraday collectors in mass spectrometry. *Rapid Commun. Mass Spectrom.* **2013**, *27*, 603–612. [CrossRef] [PubMed]
32. John, C.M.; Bowen, D. Community software for challenging isotope analysis: First applications of 'Easotope' to clumped isotopes: Community software for challenging isotope analysis. *Rapid Commun. Mass Spectrom.* **2016**, *30*, 2285–2300. [CrossRef] [PubMed]
33. Baertschi, P. Absolute^{18}O content of standard mean ocean water. *Earth Planet. Sci. Lett.* **1976**, *31*, 341–344. [CrossRef]
34. *IAEA-TECDOC—825*; Standards and Intercomparison Materials Distributed by the International Atomic Energy Agency for Stable Isotope Measurements. International Atomic Energy Agency: Vienna, Austria, 1995; pp. 13–29.
35. Meijer, H.A.J.; Li, W.J. The Use of Electrolysis for Accurate $\delta^{17}O$ and $\delta^{18}O$ Isotope Measurements in Water. *Isot. Environ. Health Stud.* **1998**, *34*, 349–369. [CrossRef]
36. Assonov, S.S.; Brenninkmeijer, C.A.M. A redetermination of absolute values for17RVPDB-CO2 and17RVSMOW. *Rapid Commun. Mass Spectrom.* **2003**, *17*, 1017–1029. [CrossRef] [PubMed]
37. Brand, W.A.; Assonov, S.S.; Coplen, T.B. Correction for the ^{17}O interference in $\delta(^{13}C)$ measurements when analyzing CO_2 with stable isotope mass spectrometry (IUPAC Technical Report). *Pure Appl. Chem.* **2010**, *82*, 1719–1733. [CrossRef]
38. Bernasconi, S.M.; Müller, I.A.; Bergmann, K.D.; Breitenbach, S.F.M.; Fernandez, A.; Hodell, D.A.; Jaggi, M.; Meckler, A.N.; Millan, I.; Ziegler, M. Reducing Uncertainties in Carbonate Clumped Isotope Analysis Through Consistent Carbonate-Based Standardization. *Geochem. Geophys. Geosystems* **2018**, *19*, 2895–2914. [CrossRef] [PubMed]
39. Daëron, M.; Blamart, D.; Peral, M.; Affek, H.P. Absolute isotopic abundance ratios and the accuracy of Δ47 measurements. *Chem. Geol.* **2016**, *442*, 83–96. [CrossRef]
40. Schauer, A.J.; Kelson, J.; Saenger, C.; Huntington, K.W. Choice of ^{17}O correction affects clumped isotope (Δ_{47}) values of CO_2 measured with mass spectrometry: ^{17}O correction affects CO_2 clumped isotopes. *Rapid Commun. Mass Spectrom.* **2016**, *30*, 2607–2616. [CrossRef] [PubMed]
41. Bernasconi, S.; Daëron, M.; Bergmann, K.D.; Bonifacie, M.; Meckler, A.N. InterCarb: A community effort to improve inter-laboratory standardization of the carbonate clumped isotope thermometer using carbonate standards. *Geochemistry* **2020**, *22*, e2020GC009588.
42. Anderson, N.T.; Kelson, J.R.; Kele, S.; Daëron, M.; Bonifacie, M.; Horita, J.; Mackey, T.J.; John, C.M.; Kluge, T.; Petschnig, P.; et al. A Unified Clumped Isotope Thermometer Calibration (0.5–1100 °C) Using Carbonate-Based Standardization. *Geophys. Res. Lett.* **2021**, *48*, e2020GL092069. [CrossRef]
43. Shen, C.-C.; Lawrence Edwards, R.; Cheng, H.; Dorale, J.A.; Thomas, R.B.; Bradley Moran, S.; Weinstein, S.E.; Edmonds, H.N. Uranium and thorium isotopic and concentration measurements by magnetic sector inductively coupled plasma mass spectrometry. *Chem. Geol.* **2002**, *185*, 165–178. [CrossRef]
44. Shen, C.-C.; Wu, C.-C.; Cheng, H.; Lawrence Edwards, R.; Hsieh, Y.-T.; Gallet, S.; Chang, C.-C.; Li, T.-Y.; Lam, D.D.; Kano, A.; et al. High-precision and high-resolution carbonate 230Th dating by MC-ICP-MS with SEM protocols. *Geochim. Cosmochim. Acta* **2012**, *99*, 71–86. [CrossRef]
45. Cheng, H.; Lawrence Edwards, R.; Shen, C.-C.; Polyak, V.J.; Asmerom, Y.; Woodhead, J.; Hellstrom, J.; Wang, Y.; Kong, X.; Spötl, C.; et al. Improvements in 230Th dating, 230Th and 234U half-life values, and U–Th isotopic measurements by multi-collector inductively coupled plasma mass spectrometry. *Earth Planet. Sci. Lett.* **2013**, *371–372*, 82–91. [CrossRef]
46. Kele, S.; Breitenbach, S.F.M.; Capezzuoli, E.; Meckler, A.N.; Ziegler, M.; Millan, I.M.; Kluge, T.; Deák, J.; Hanselmann, K.; John, C.M.; et al. Temperature dependence of oxygen- and clumped isotope fractionation in carbonates: A study of travertines and tufas in the 6–95 °C temperature range. *Geochim. Cosmochim. Acta* **2015**, *168*, 172–192. [CrossRef]
47. Panichi, C.; Tongiorgi, E. Carbon isotopic composition of CO_2 from springs, fumaroles, mofettes and travertines of central and southern Italy: A preliminary prospection method of geothermal areas. In Proceedings of the 2nd United Nations Symposium on the Development and Use of Geothermal Resources, San Francisco, CA, USA, 20 May 1975.
48. Bačová, N.; Nemeth, Z.; Repčiak, M. Mineral Waters of the Dudince Spa. *Slovak Geol. Mag.* **2016**, *16*, 125–147.
49. Holko, L.; Dóša, M.; Michalko, J.; Šanda, M. Isotopes of oxygen-18 and deuterium in precipitation in Slovakia/Izotopy kyslíka-18 A deutéria v zrážkach na Slovensku. *J. Hydrol. Hydromech.* **2012**, *60*, 265–276. [CrossRef]
50. Craig, H. Standard for reporting concentrations of deuterium and oxygen-18 in natural waters. *Science* **1961**, *133*, 1833–1834. [CrossRef]
51. Petrbok, J. Mekkýši travertinù slovenského Krasu, Gánovcù s okolím, Spiše a Ružbachù. *Rozpr. II. Tøídy Èeské Akad.* **1937**, *46*, 1–16.
52. Ložek, V.; Prošek, F. Krasové zjevy v travertinech a jejich statigrafický význam. *Československý Kras* **1957**, *10*, 145–158.
53. Del Tredici, P. Ginkgos and multituberculates: Evolutionary interactions in the Tertiary. *Biosystems* **1989**, *22*, 327–339. [CrossRef] [PubMed]

54. Ložek, V. Nové interglaciální malakofauny ze Slovenska. (Neue interglaziale Molluskenfaunen in der Slowakei). *Anthropozoikum* **1958**, *7*, 37–45.
55. Holec, P. Teeth casts of Mastodont species Mammut borsoni (Hays, 1834) from the Dreveník travertine near Spišské Podhradie. *Miner. Slovaca* **1992**, *24*, 467–469.
56. Fordinál, K.; Nagy, A. Hlavina member—Marginal Upper Pannonian sediments of the Rišňovce depression. *Miner. Slovaca* **1997**, *29*, 401–406.
57. Kaminská, L. Príspevok k poznaniu micoquienu na Slovensku. In *Ecce Homo, in Memoriam Jan Fridrich*; Krigl Jan: Praha, Czech Republic, 2010; pp. 90–94. ISBN 9788086912455.
58. Tóth, C.; Krempaská, Z. Pliocene Proboscidea remains from travertine Dreveník site (near Spišské Podhradie, Slovakia). In Proceedings of the 6th Meeting of The European Association of Vertebrate Palaeontologists, Spišská Nová Ves, Slovakia, 30 June–5 July 2008; p. 116.
59. Nemergut, A. Sídlisková Geografia Považia a Ponitria v Staršej Dobe Kamennej. Ph.D. Thesis, Masarykova Univerzita v Brně, Brno, Czech Republic, 2011.
60. Wróblewski, W.; Gradziński, M.; Hercman, H. Suggestions on the allochthonous origin of terra rossa from Drevenik Hill (Spiš, Slovakia). *Slov. Kras* **2010**, *48*, 153–161.
61. Kovanda, J.; Smolíkovà, L.; Ford, D.; Kaminská, L.; Ložek, V.; Horácek, I. The Skalka travertine mound at Hôrce-Ondrej near Poprad (Slovakia). *Sborník Geol. Ved–Antropozoikum* **1995**, *22*, 113–140.
62. Frank, N.; Braum, M.; Hambach, U.; Mangini, A.; Wagner, G. Warm Period Growth of Travertine during the Last Interglaciation in Southern Germany. *Quat. Res.* **2000**, *54*, 38–48. [CrossRef]
63. Rihs, S.; Condomines, M.; Poidevin, J.-L. Long-term behaviour of continental hydrothermal systems. *Geochim. Cosmochim. Acta* **2000**, *64*, 3189–3199. [CrossRef]
64. Soligo, M.; Tuccimei, P.; Barberi, R.; Delitala, M.C.; Miccadei, E.; Taddeucci, A. U/Th dating of freshwater travertine from Middle Velino Valley (Central Italy): Paleoclimatic and geological implications. *Palaeogeogr. Palaeoclimatol. Palaeoecol.* **2002**, *184*, 147–161. [CrossRef]
65. Lisiecki, L.E.; Raymo, M.E. A Pliocene-Pleistocene stack of 57 globally distributed benthic $\delta^{18}O$ records. *Paleoceanography* **2005**, *20*, 9–11. [CrossRef]
66. Gradziński, M.; Hercman, H.; Jaśkiewicz, M.; Szczurek, S. Holocene tufa in the Slovak Karst: Facies, sedimentary environments and depositional history. *Geol. Q.* **2013**, *57*, 769–788. [CrossRef]
67. Clark, P.U.; Dyke, A.S.; Shakun, J.D.; Carlson, A.E.; Clark, J.; Wohlfarth, B.; Mitrovica, J.X.; Hostetler, S.W.; McCabe, A.M. The last glacial maximum. *Science* **2009**, *325*, 710–714. [CrossRef]
68. Bertini, A.; Minissale, A.; Ricci, M. Use of Quaternary travertines of central-southern Italy as archives of paleoclimate, paleohydrology and neotectonics. *Alp. Mediterr. Quat.* **2008**, *21*, 99–112.
69. Ricketts, J.W.; Ma, L.; Wagler, A.E.; Garcia, V.H. Global travertine deposition modulated by oscillations in climate. *J. Quat. Sci.* **2019**, *34*, 558–568. [CrossRef]
70. Uysal, I.T.; Feng, Y.-X.; Zhao, J.-X.; Isik, V.; Nuriel, P.; Golding, S.D. Hydrothermal CO_2 degassing in seismically active zones during the late Quaternary. *Chem. Geol.* **2009**, *265*, 442–454. [CrossRef]
71. Pentecost, A.; Viles, H. A review and reassessment of travertine classification. *Géogr. Phys. Quat.* **1994**, *48*, 305–314. [CrossRef]
72. Gandin, A.; Capezzuoli, E. Travertine versus calcareous tufa: Distinctive petrologic features and stable isotopes signatures. *Alp. Mediterr. Quat.* **2008**, *21*, 125–136.
73. Berardi, G.; Vignaroli, G.; Billi, A.; Rossetti, F.; Soligo, M.; Kele, S.; Baykara, M.O.; Bernasconi, S.M.; Castorina, F.; Tecce, F.; et al. Growth of a Pleistocene giant carbonate vein and nearby thermogene travertine deposits at Semproniano, southern Tuscany, Italy: Estimate of CO_2 leakage. *Tectonophysics* **2016**, *690*, 219–239. [CrossRef]
74. Della Porta, G.; Hoppert, M.; Hallmann, C.; Schneider, D.; Reitner, J. The influence of microbial mats on travertine precipitation in active hydrothermal systems (Central Italy). *Depos. Rec.* **2022**, *8*, 165–209. [CrossRef]
75. Kele, S.; Özkul, M.; Fórizs, I.; Gökgöz, A.; Baykara, M.O.; Alçiçek, M.C.; Németh, T. Stable isotope geochemical study of Pamukkale travertines: New evidences of low-temperature non-equilibrium calcite-water fractionation. *Sediment. Geol.* **2011**, *238*, 191–212. [CrossRef]
76. Özkul, M.; Kele, S.; Gökgöz, A.; Shen, C.-C.; Jones, B.; Baykara, M.O.; Fórizs, I.; Németh, T.; Chang, Y.-W.; Alçiçek, M.C. Comparison of the Quaternary travertine sites in the Denizli extensional basin based on their depositional and geochemical data. *Sediment. Geol.* **2013**, *294*, 179–204. [CrossRef]
77. Kele, S.; Vaselli, O.; Szabó, C.; Minissale, A. Stable isotope geochemistry of Pleistocene travertine from Budakalász (Buda Mts, Hungary). *Acta Geol. Hung.* **2003**, *46*, 161–175. [CrossRef]
78. Hoefs, J. *Stable Isotope Geochemistry*; Springer: Berlin/Heidelberg, Germany, 1997.
79. Cornides, I.; Kecskés, Á. Deep-seated carbon dioxide in Slovakia: The problem of its origin. *Geol. Carpathica* **1982**, *33*, 183–190.
80. Cornides, I.; Kecskes, A. Deep-seated carbon dioxide in Slovakia: Additional comments on the problem of its origin. *Geol. Zb.* **1987**, *38*, 429–435.
81. Cornides, I.; Takaoka, N.; Nagao, K.; Matsuo, S. Contribution of mantle-derived gases to subsurface gases in a tectonically quiescent area, the Carpathian Basin, Hungary revealed by noble gas measurements. *Geochem. J.* **1986**, *20*, 119–125. [CrossRef]

82. Clark, I.D.; Fritz, P. *Environmental Isotopes in Hydrogeology*; CRC Press/Lewis Publishers: Boca Raton, FL, USA, 1997.
83. Trček, B.; Albrecht, L. Overview of isotopic investigations of groundwaters in a fractured aquifer system near Rogaška Slatina, Slovenia. *Geologija* **2017**, *60*, 49–60. [CrossRef]
84. Franko, O.; Šivo, A.; Richtáriková, M.; Povinec, P.P. Radiocarbon Ages of Mineral and Thermal Waters of Slovakia. *Acta Phys. Univ. Comen.* **2008**, *49*, 111–124.